Supplementary Materials for

Chromatin decondensation is sufficient to alter nuclear organization in embryonic stem cells

Pierre Therizols, Robert S. Illingworth, Celine Courilleau, Shelagh Boyle, Andrew J. Wood, Wendy A. Bickmore*

*Corresponding author. E-mail: wendy.bickmore@igmm.ed.ac.uk

Published 5 December 2014, *Science* **346**, 1238 (2014)
DOI: 10.1126/science.1259587

This PDF file includes:

Materials and Methods

TALE design and assembly tPtn transcription factors were assembled using methods previously described (*10*). Briefly, a TALE DNA binding domain specific for 14 nucleotide sequences within the *Ptn* promoter was generated by the modular assembly of individual TALE repeats using golden gate cloning technology and inserted into a backbone vector containing VP64, a nuclear localization signal (NLS) and the N- and C-termini of a naturally occurring TALE protein (hax3 from *Xanthomonas campestris*) to generate tPtn-VP64. The NheI-XbaI fragment containing NLS-VP64 was replaced by PCR products encoding either an NLS or NLS-DELQPASIDP (*13*) to generate tPtn-Δ and tPtn-DEL, respectively. TALE DNA binding domains specific to the *Sox6* and *Nrp1* promoters were assembled following the methods described in (*11*). Briefly, DNA binding domains specific for 16 nucleotide sequences were generated by the modular assembly of 4 pre-assembled multimeric TALE repeat modules (three 4-mer and one 3-mer) into a modified TALEN backbone in which the BamHI-BsrGI fragment containing hFokI2-2A-eGFP was replaced by a gBlocks® (IDT) fragment encoding VP64-2A-eGFP. The BamHI-BglII fragment containing VP64 of tNrp1-VP64 and tSox6-VP64 was deleted to generate tNrp1-Δ and tSox6-Δ, respectively. The BamHI-NheI fragment containing VP64 of tNrp1-VP64 and tSox6-VP64 was replaced by double strand oligonucleotide encoding a DELQPASIDP peptide (*13*) to generate tNrp1-DEL and tSox6-DEL, respectively. Target sequences for the TALE repeat domains used are shown in Fig. 1A.

Cell culture E14 ES cells (ESCs) were grown in GMEM supplemented with 15% fetal bovine serum (FBS), 1,000 units/ml LIF, nonessential amino acids, sodium pyruvate, 2-β-mercaptoethanol, L-glutamine, and Penicillin/Streptomycin. ESCs were differentiated in neural progenitor cells (NPCs) by growing for 2 days with retinoic acid following the protocol described in (*19*), followed by 2 days in N2B27 medium (*20*). EpiSC were derived from E14 cells and cultured as described (*21*). ESCs were transfected with plasmids using Lipofectamine® 2000 Reagent (Invitrogen cat. N°11668) following the manufacturer recommendations. Briefly, $1x10^6$ ESCs were transfected in a 6-well plate with 3µg of plasmid and 7µl of lipofectamin. Medium was changed 5h after transfection. Transfected cells were sorted based on eGFP expression by FACS 24h after transfection and re-seeded for another 24h before harvesting for experiments.

Flow Cytometric Analysis To sort GFP positive cells, cells were trypsinized and resuspended in FACS buffer (PBS and 10% medium) at $3x10^6$ cells/ml. For cell cycle analysis, cells were fixed in 70% EtOH with gentle vortexing and then stained with 50 µg/ml propidium iodide (PI) for 30 min in the presence of 0.5 mg/ml RNaseA. Flow cytometric analysis was performed using a BD FACSAriaII SORP (Becton Dickinson). The 488nm laser was used to measure eGFP and the PI fluorescence with 525/50 nm and 685/35 nm bandpass filters, respectively. BD FACSDiva software (Becton Dickinson, Version 6.1.2) was used for instrument control and data analysis.

FISH Nuclei were isolated in hypotonic buffer (0.25% KCl, 0.5% tri-sodium citrate) and fixed with 3:1 v/v methanol/acetic acid. Fosmid clones (Table S2) were prepared and labelled with digoxigenin-11-dUTP or with biotin-16-dUTP as previously described (*19*). Approximately 150 ng of biotin- and digoxigenin-labelled fosmid probes were used per

slide, together with 15 μg of mouse Cot1 DNA (GIBCO BRL) and 10 μg salmon sperm DNA. Probes were denatured at 70°C for 5 min, reannealed with CotI DNA for 15 min at 37°C and hybridized to the denatured slides overnight. Washes and detection were as described previously (*19, 22*).

Image Capture and Analysis Slides were examined on a Zeiss Axioplan II fluorescence microscope fitted with Plan-neofluar objectives, a 100 W Hg source (Carl Zeiss, Welwyn Garden City, UK) and Chroma #83000 triple band pass filter set (Chroma Technology Corp., Rockingham, VT) with the excitation filters installed in a motorised filter wheel (Prior Scientific Instruments, Cambridge, UK). Images were captured with a Coolsnap HQ CCD camera (Photometrics Ltd, Tucson, AZ). Image capture and analysis were performed using in-house scripts written for iVision (BioVision Technologies, Inc, Exton, PA). The radial positions of loci were determined as previously described (*23*) by radial analysis of 100–150 nuclei, using five shells of equal area eroded from the periphery (shell 1) through to the center (shell 5) of the nucleus (Fig. S1). The statistical significance of differences in radial positioning was assessed using chi^2 test to examine the null hypothesis that the locus exhibits the same radial distribution in the 2 experiments.

Chromatin condensation was assayed as described previously (*14*). To normalize distances for changes in nuclear size, squared interprobe distances (d^2) $(\mu m)^2$ were normalized to nuclear radius^2 (r^2). Nuclear area was measured from the DAPI signal and the radius calculated assuming the nuclei to be circular (Area = πr^2). The statistical significance of differences in mean-squared interprobe distances was assessed using the nonparametric Mann-Whitney U test to examine the null hypothesis. Each data set consisted of at least 100 nuclei (200 loci) for each cell line unless other stated, and for each combination of probes.

RNA extraction and cDNA first strand synthesis RNA was prepared using an RNeasy mini kit (Qiagen) according to the manufacturer's protocol, including a DNaseI (Qiagen) treatment for 15 min at room temperature. cDNA was synthesized from 5 μg purified RNA with Superscript II reverse transcriptase (Invitrogen) primed with random hexamers (Promega).

Real-Time PCR Real-time PCR was carried on a Roche LightCycler 480 Real-Time PCR System using a Lightcycler 480 Sybr Green detection kit (Roche). The real-time thermal cycler was programmed as follows: 15 min Hotstart; 44 PCR cycles (95°C for 15 s, 55°C for 30 s, 72°C for 30 s). For transcript analysis, a standard curve for each primer set (Table S3) was obtained using a mix of each of the cDNAs. The relative expression of each sample was measured by the Lightcycler software and normalized to the mean for *Gapdh* from 3 biological replicates. Finally, the log2 of the ratio relative to eGFP transfected ESCs was calculated.

Gene expression microarray 1μg of purified RNA was mixed with RNA standards (One Colour RNA Spike-In Kit; Agilent – 5188-5282) and the mixture labelled with cyanine 3 (Cy3) using the Amino Allyl MessageAmp™ II with Cy™3 kit (Ambion; AM1795) according to manufacturer's instructions. 600 ng of labeled RNA were hybridized to a SurePrint G3 Mouse GE 8x60K microarray (Agilent; G4852A). RNA quantification and

integrity was monitored throughout using the total RNA nano chip measured on an Agilent Bioanalzer. Microarrays were hybridized for 17 hours, washed according to the manufacturer's instructions and scanned on a Nimblegen scanner at 2 μm resolution. The resulting single channel TIFF images was processed using feature extraction software (Agilent).

Raw intensity values were averaged across replicated probes (where applicable), normalized and then combined using the limma package in R. Genes with a p value <0.01 following Bayesian modeling and multiple testing correction (*24*) were considered as differentially expressed. Microarray data is deposited in the GEO repository (http://www.ncbi.nlm.nih.gov/geo/; accession: GSE62379).

Chromatin Immunoprecipitation Harvested ESCs ($0.5 – 1.5x10^7$) were fixed in media by the addition of an equal volume of 2% methanol-free formaldehyde (Thermo Scientific Pierce PN28906; final concentration of 1%) and incubation at RT for 10 min followed by 5 min incubation with 125mM glycine at room temperature. Cells were then washed in PBS. All buffers were supplemented with the following additives just prior to use (0.2 mM PMSF, 1 mM DTT, 1x Protease inhibitors (Calbiochem, 539134-1SET) and 1x phosphatase inhibitors (Roche, PhosSTOP, 04906837001)). Cell pellets were resuspended in lysis buffer 1 (50mM Tris-HCl pH 8.1, 10mM EDTA, 20% SDS) and incubated for 10 min at 4°C. Lysates were diluted 1:10 in ChIP dilution buffer (0.1% Triton X-100, 2mM EDTA, 150mM NaCl, 20mM Tris-HCl pH8.1) and sonicated using a bioruptor (Diagenode) at 4°C for 15 cycles of 30 sec (30 sec pause between pulses) set to high. The sonicated extract was centrifuged at 16000 *g* for 10 min at 4°C and the supernatant transferred to a fresh tube and supplemented with BSA and Triton X-100 to final concentrations of 25μg/ml and 1% respectively. 5% of the chromatin was retained as an input reference and the remainder incubated overnight at 4ºC on a rotating wheel with anti-RNAPII subunit B1 antibodies (clone 8WG; 05-952, Millipore) pre-coupled to protein G or Sheep Anti-Rat IgG Dynabeads respectively (Life Technologies; 10004D and 11035 respectively; 10 μg of antibody bound to 40μl of stock dynabeads per IP). Bead-associated immune complexes were washed sequentially with wash buffers A, B and C each for 2 x 5 mins at 4ºC on a rotating wheel followed by 2 washes in TE buffer at RT (wash buffer A - 1% Triton X-100, 2mM EDTA, 150mM NaCl, 20mM Tris-HCl pH8.1; wash buffer B - 1% Triton X-100, 0.1% Sodium-Deoxycolate, 0.1% SDS, 1mM EDTA, 500mM NaCl, 20mM Tris-HCl pH8.1; wash buffer C – 1% NP40, 0.1% Sodium-Deoxycolate, 1mM EDTA, 250mM LiCl, 20mM Tris-HCl pH8.1). Chromatin was released from the beads by incubation with elution buffer (0.1 M NaHCO3, 1 % SDS) for 15 mins at 37 ºC. RNaseA and Tris pH6.8 were added to final concentrations of 20mg/ml and 100mM respectively, and incubation carried out at 65ºC for 2 hours. 50μg of proteinase K were added and incubation at 65ºC continued for 8 hours to degrade proteins and reverse the cross-links. Purified DNA was isolated using QIAquick PCR Purification Kit (Qiagen). Quantitative PCR was performed on a LightCycler480 (Roche) using the LighCycler sybr green master mix (Roche) according to the manufacturer's instructions.

Replication timing analysis Samples were prepared by adaptation of a published method (*25*). BrdU was added to ESC medium to 50μM final concentration and incubated for 1h

at 37°C and 5% CO_2. Cells were trypsinized, fixed in 70% EtOH, stained with 50 µg/ml PI for 30 min in the presence of RNaseA (0.5 mg/ml) and then sorted by FACS into early and late S-phase fractions. BrdU labeled DNA was immuno-precipitated in IP buffer (10 mM sodium phosphate pH 7.0, 140 mM NaCl, 0.05% Triton X-100) using 0.5µg of anti-BrdU antibody (B&D) pre-bound to Protein G dynabeads (Invitrogen). Beads were washed 3 times with IP buffer. Bound complexes were eluted from beads in lysis buffer (Tris-HCl 50 mM pH8, EDTA 10 mM pH8, 1% SDS and proteinase K 0.2 mg/ml) for 2h at 56°C. Immuno-precipitated and input DNA were purified with Qiagen PCR purification kit. A percentage input (%IP) was calculated for each primer set (Table S3) for the early and late fractions using the formula: $\%IP=2^{(Ct\ IN - Ct\ IP)}$. Where Ct IN is the corrected Ct value obtained for the 10% input and Ct IP is the Ct value of the immuno-precipitated fraction. The log2 of the ratio $\%IP_{early}$ over $\%IP_{late}$ was calculated.

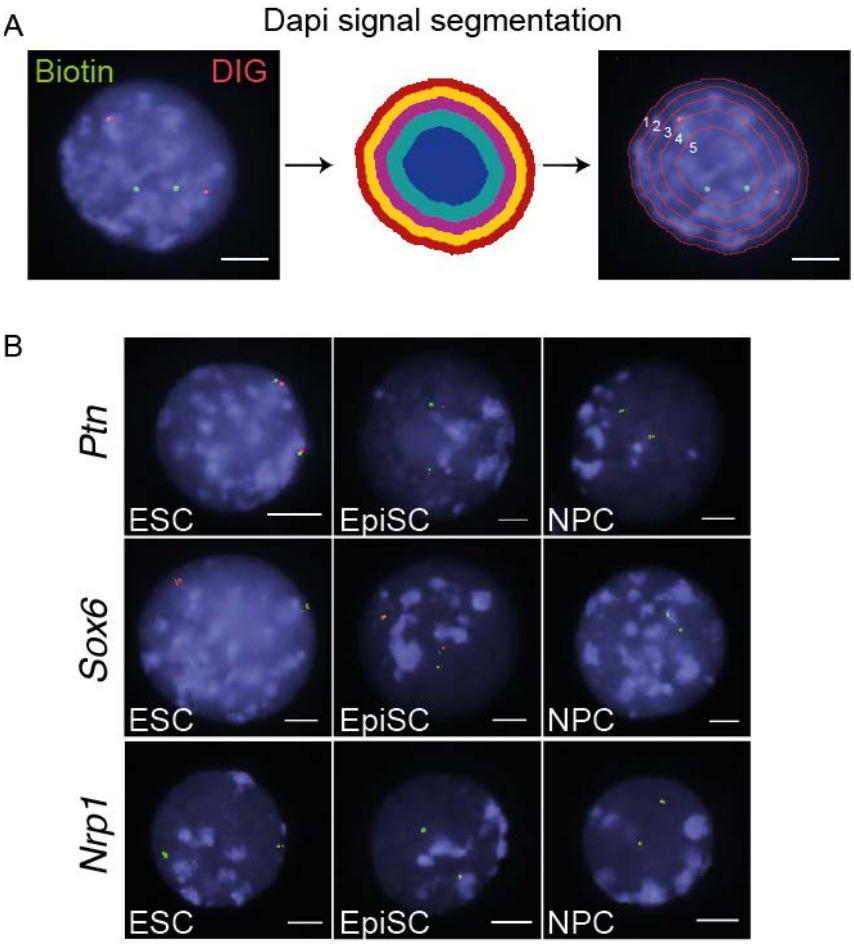

Fig. S1.

Radial positioning analysis. (A) Schematic of radial positioning assay. FISH with probes labeled with biotin-16-dUTP (green) and digoxigenin-11-dUTP (red), in fixed nuclei of E14 ESCs counter- stained with DAPI (blue). Scale bar = 5µm). The erosion analysis script segmented the DAPI signal in five shells of equal area eroded from the periphery (shell 1) through to the center (shell 5) of the nucleus. Regions of interest (ROIs) were then defined manually around the probe signals, segmented and the signal intensity weighted centroid coordinates calculated. Finally, positions of the centroids across the 5 erosion shells was then determined. (B) FISH with probes hybridizing to *Ptn* (top), *Sox6* (middle), and *Nrp1* (bottom) in nuclei of ESCs (left), and ESCs differentiated into EpiSCs (center) and NPCs (right). Nuclei were counter- stained with DAPI (blue). Scale bar = 5 µm.

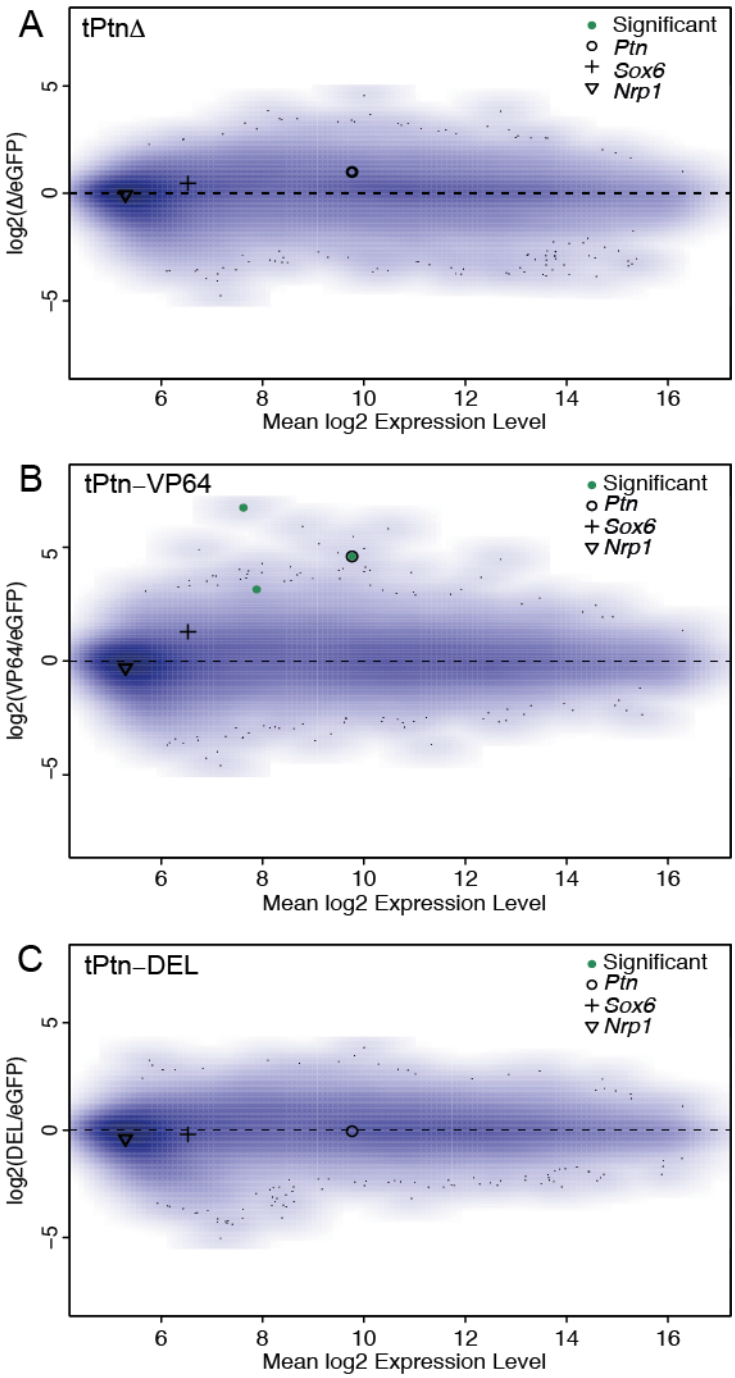

Fig. S2

Limited off-targets of tPtn TALEs. MA plots of gene expression microarray analysis for ESCs transfected by tPtn-Δ (top), tPtn-VP64 (center) and tPtn-DEL (bottom). A circle, cross and triangle represent *Ptn*, *Sox6* and *Nrp1* respectively. A green circle represents significant changes in expression compare to ESCs transfected by eGFP.

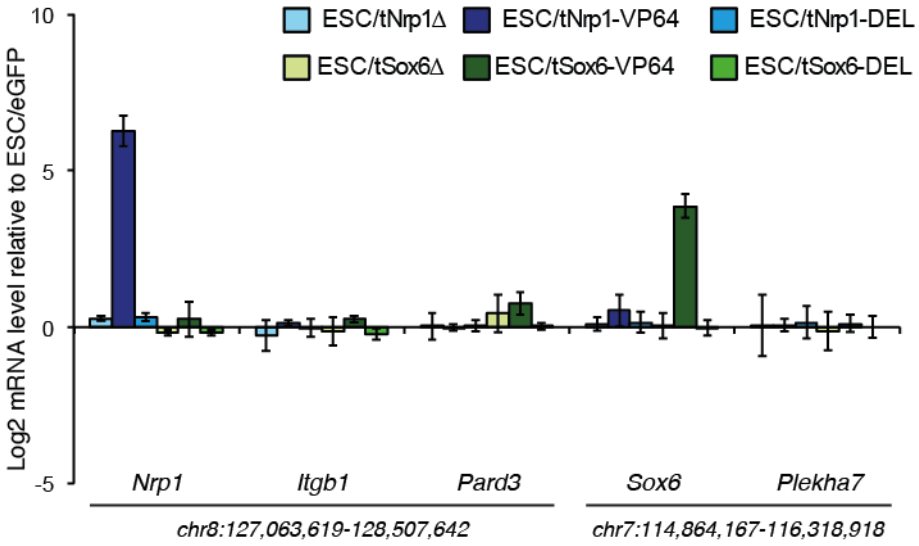

Fig. S3

tNrp1 and tSox6 TALEs do not affect neighboring genes. Mean (+/- s.e.m.) log2 mRNA level, established by RT-qPCR, for the TALEs target genes (*Nrp1*, *Sox6*), and genes located within 1Mb of these genes (*Itgb1*, *Pard3*, *Plekha7*) in ESCs transfected with the different TALEs vectors. Expression is shown relative to cells transfected with eGFP. n = 2 biological replicates. Genomic co-ordinates are from the mm10 version of the mouse genome assembly. The Ptn locus is located ay Chr6: 36,714,929-36,715,535.

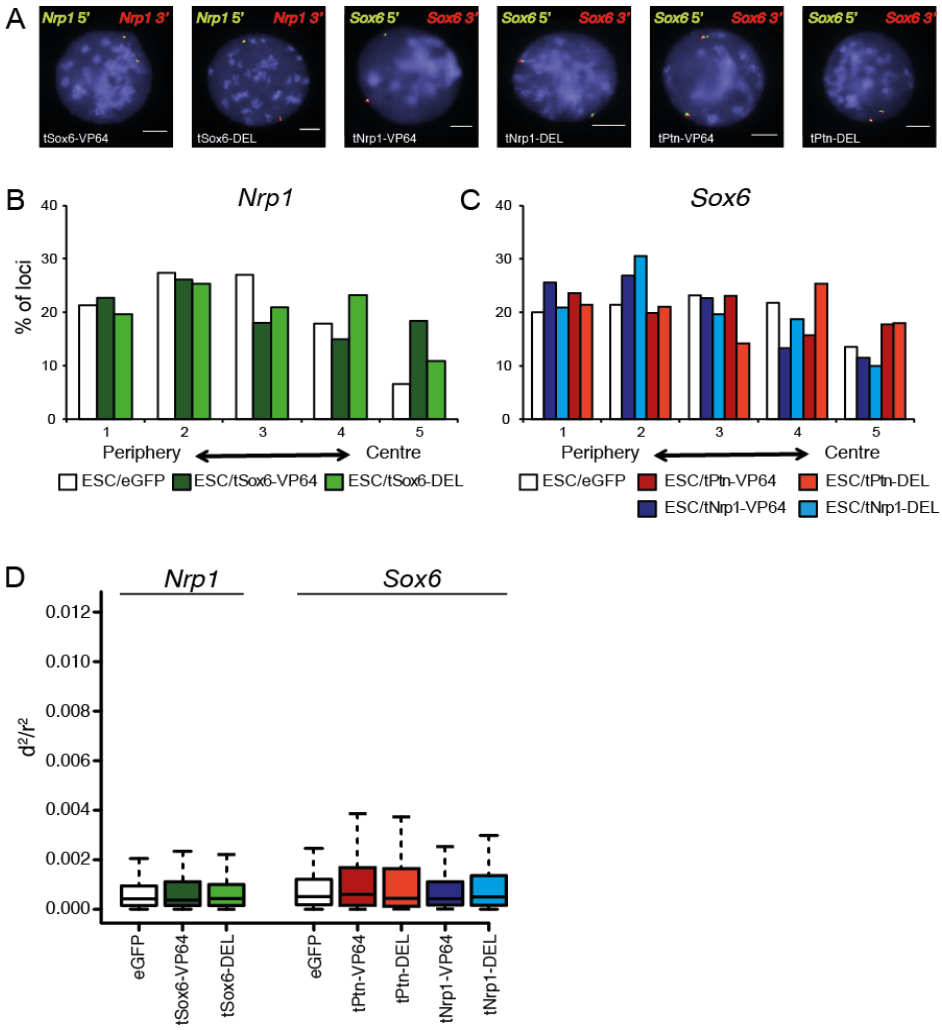

Figure. S4.

Effects of TALEs on radial positioning and chromatin condensation are limited to the targeted region. (A) FISH with probe pairs either side of *Nrp1* (Nrp1 5' and 3') and *Sox6* (Sox6 5' and 3'), in nuclei of ESCs transfected by the different TALEs, from left to right: tSox6-VP64, tSox6-DEL, tNrp1-VP64, tNrp1-DEL, tPtn-VP64 and tPtn-DEL. Scale bar = 5 µm. (B) Histograms show the distribution of *Nrp1* hybridization signals across 5 concentric shells eroded from the periphery (shell 1) through to the center (shell 5) of the nucleus (Fig. S1) in ESCs transfected by eGFP (white), tSox6-VP64 (dark green) and tSox6-DEL (green). At least 2 biological replicates were performed, each comprising 100-150 nuclei. (C) As in (B) but for the distribution of *Sox6* hybridization signals in ESCs transfected by eGFP (white), tPtn-VP64 (dark red), tPtn-DEL (red), tNrp1-VP64 (dark blue) and tNrp1-DEL (blue). (D) Box plots showing the distribution of interprobe distances^2 (d^2) normalized for nuclear radius^2 (r^2) at *Nrp1* (left), and *Sox6* (right) in ESCs transfected by eGFP, tSox6-VP64 (dark green), tSox6-DEL (green), tPtn-VP64 (dark red), tPtn-DEL (red), tNrp1-VP64 (dark blue) and tNrp1-DEL (blue). The shaded boxes show the median and interquartile range of the data. n = 100-150 nuclei. The statistical significance of differences between ESCs/eGFP and other conditions were examined by Mann-Whitney U tests (Table S1).

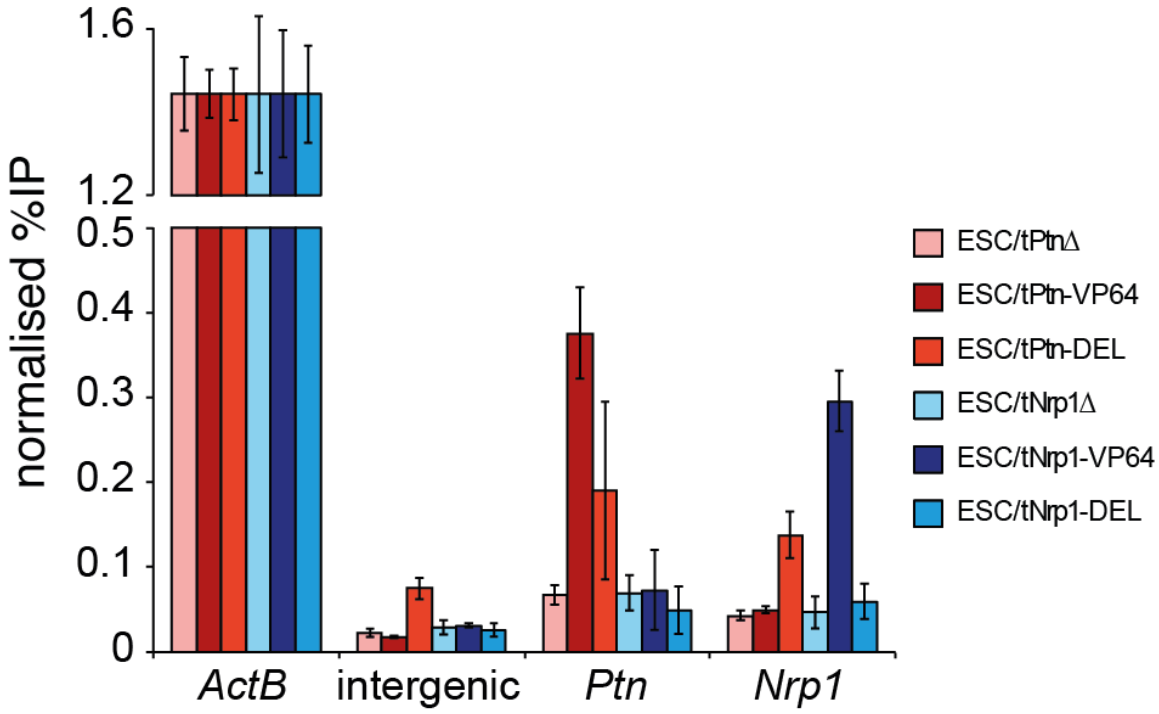

Figure. S5.
DELQPASIDP peptide does not recruit the transcription machinery. Second biological replicate of the ChIP for RNAPII (8WG) at the promoters of *Actb*, *Ptn*, *Nrp1* and at an intergenic negative control, assayed by qPCR, in ESC transfected by tPtn-Δ (light red), tPtn-VP64 (dark red), tPtn-DEL (red), tNrp1-Δ (light blue), tNrp1-VP64 (dark blue), tNrp1-DEL (blue). Enrichment is shown as mean % input bound ± SD over three technical replicates.

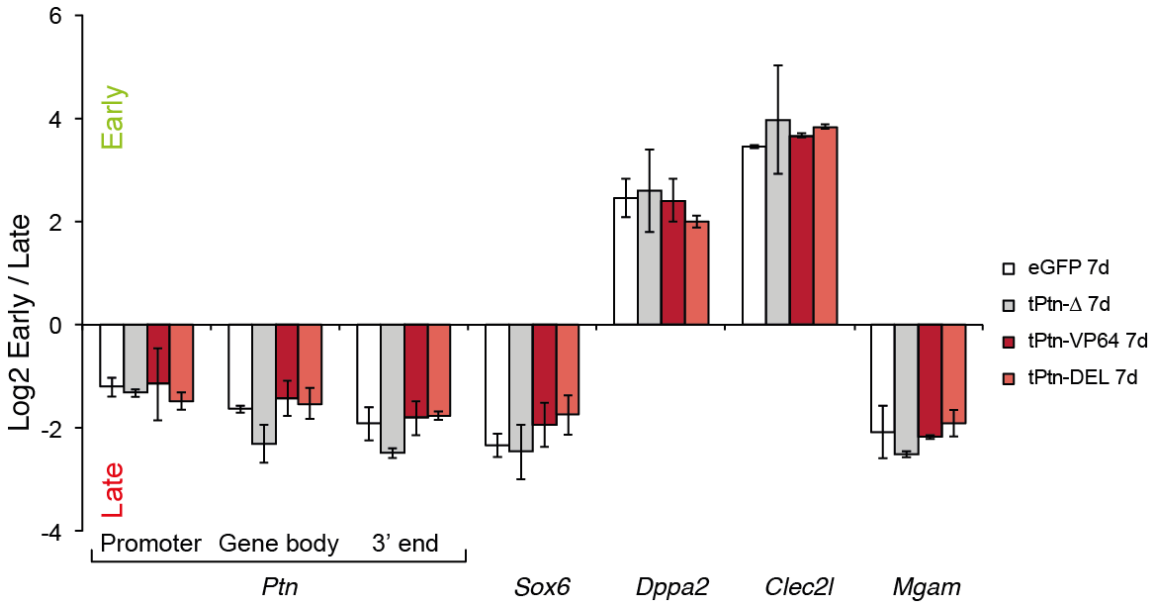

Figure. S6.
Replication timing shift is not maintained after the loss of synthetic activation
Histograms showing the mean (+/- s.e.m.) log2 ratio of early: late S phase fraction, as established by real-time PCR measurement of the percentage of input bound. Presented are *Ptn* (3 sets of primers: promoter, gene body and 3' end), *Sox6*, *Dppa2*, *Clec2l* and *Mgam*, in ESCs 7 days after transfection with eGFP (white), tPtn-Δ (light gray), tPtn-VP64 (dark red) and tPtn-DEL (light red).

Table S1.

Normalized Interprobe FISH Distances and statistical analysis. Nd= not determined

Normalized interprobe distance (d^2/r^2)		*Ptn*	*Sox6*	*Nrp1*
	ESC / eGFP	6.98E-04	5.10E-04	4.18E-04
	ESC / tPtn-Δ	9.73E-04	7.34E-04	Nd
Mann-Whitney Test		p = 0.23	p = 0.39	Nd
	ESC / eGFP	6.98E-04	5.10E-04	4.18E-04
	ESC / tPtn-VP64	1.94E-03	6.00E-04	Nd
Mann-Whitney Test		p = 1.23E-07	p = 0.63	Nd
	ESC / eGFP	6.98E-04	5.10E-04	4.18E-04
	ESC / tPtn-DEL	1.89E-03	4.46E-04	Nd
Mann-Whitney Test		p = 2.37E-06	p = 0.46	Nd
	ESC / eGFP	6.98E-04	5.10E-04	4.18E-04
	EpiSC	1.77E-03	1.50E-03	Nd
Mann-Whitney Test		p = 5.71E-07	p = 4.41E-09	Nd
	ESC / tPtn-Δ	9.73E-04	7.34E-04	Nd
	ESC / tPtn-VP64	1.94E-03	6.00E-04	Nd
Mann-Whitney Test		p = 9.55E-06	p = 0.92	Nd
	ESC / tPtn-Δ	9.73E-04	7.34E-04	Nd
	ESC / tPtn-DEL	1.89E-03	4.46E-04	Nd
Mann-Whitney Test		p = 1.91E-04	p = 0.27	Nd
	ESC / tPtn-Δ	9.73E-04	7.34E-04	Nd
	EpiSC	1.77E-03	1.50E-03	Nd
Mann-Whitney Test		p = 6.31E-05	p = 1.01E-06	Nd
	ESC / tPtn-VP64	1.94E-03	6.00E-04	Nd
	ESC / tPtn-DEL	1.89E-03	4.46E-04	Nd
Mann-Whitney Test		p = 0.42	p = 0.34	Nd
	ESC / tPtn-VP64	1.94E-03	6.00E-04	Nd
	EpiSC	1.77E-03	1.50E-03	Nd
Mann-Whitney Test		p = 0.59	p = 9.89E-07	Nd
	ESC / tPtn-DEL	1.89E-03	4.46E-04	Nd
	EpiSC	1.77E-03	1.50E-03	Nd
Mann-Whitney Test		p = 0.85	p = 1.15E-09	Nd
	ESC / eGFP	6.98E-04	5.10E-04	4.18E-04
	ESC / tSox6-Δ	Nd	4.43E-04	Nd
Mann-Whitney Test		Nd	p = 0.22	Nd
	ESC / eGFP	6.98E-04	5.10E-04	4.18E-04
	ESC / tSox6-VP64	Nd	1.41E-03	3.73E-04
Mann-Whitney Test		Nd	p = 4.29E-09	p = 0.79

	ESC / eGFP	6.98E-04	5.10E-04	4.18E-04
	ESC / tSox6-DEL	Nd	1.00E-03	4.33E-04
Mann-Whitney Test		Nd	p = 3.58E-06	p = 0.55
	ESC / tSox6-Δ	Nd	4.43E-04	Nd
	ESC / tSox6-VP64	Nd	1.41E-03	3.73E-04
Mann-Whitney Test		Nd	p = 9.04E-13	Nd
	ESC / tSox6-Δ	Nd	4.43E-04	Nd
	ESC / tSox6-DEL	Nd	1.00E-03	4.33E-04
Mann-Whitney Test		Nd	p = 4.98E-09	Nd
	ESC / tSox6-Δ	Nd	4.43E-04	Nd
	EpiSC	Nd	1.50E-03	Nd
Mann-Whitney Test		Nd	p = 1.50E-12	Nd
	ESC / tSox6-VP64	Nd	1.41E-03	3.73E-04
	ESC / tSox6-DEL	Nd	1.00E-03	4.33E-04
Mann-Whitney Test		Nd	p = 0.22	p = 0.78
	ESC / tSox6-VP64	Nd	1.41E-03	3.73E-04
	EpiSC	Nd	1.50E-03	Nd
Mann-Whitney Test		Nd	p = 0.63	Nd
	ESC / tSox6-DEL	Nd	1.00E-03	4.33E-04
	EpiSC	Nd	1.50E-03	Nd
Mann-Whitney Test		Nd	p = 0.11	Nd
	ESC / eGFP	6.98E-04	5.10E-04	4.18E-04
	ESC / tNrp1-Δ	Nd	Nd	4.38E-04
Mann-Whitney Test		Nd	Nd	p = 0.32
	ESC / eGFP	6.98E-04	5.10E-04	4.18E-04
	ESC / tNrp1-VP64	Nd	4.20E-04	1.28E-03
Mann-Whitney Test		Nd	p = 0.3	p < 2.2e-16
	ESC / eGFP	6.98E-04	5.10E-04	4.18E-04
	ESC / tNrp1-DEL	Nd	4.97E-04	8.58E-04
Mann-Whitney Test		Nd	p = 0.71	p = 6.07E-10
	ESC / tNrp1-Δ	Nd	Nd	4.38E-04
	ESC / tNrp1-VP64	Nd	4.20E-04	1.28E-03
Mann-Whitney Test		Nd	Nd	p < 2.2e-16
	ESC / tNrp1-Δ	Nd	Nd	4.38E-04
	ESC / tNrp1-DEL	Nd	4.97E-04	8.58E-04
Mann-Whitney Test		Nd	Nd	p = 8.64E-08
	ESC / tNrp1-Δ	Nd	Nd	4.38E-04
	EpiSC	Nd	1.50E-03	Nd
Mann-Whitney Test		Nd	Nd	Nd
	ESC / tNrp1-VP64	Nd	4.20E-04	1.28E-03
	ESC / tNrp1-DEL	Nd	4.97E-04	8.58E-04

Mann-Whitney Test		Nd	$p = 0.52$	$p = 0.004$
	ESC / tNrp1-VP64	Nd	4.20E-04	1.28E-03
	EpiSC	Nd	1.50E-03	Nd
Mann-Whitney Test		Nd	$p = 6.04E-12$	Nd
	ESC / tNrp1-DEL	Nd	4.97E-04	8.58E-04
	EpiSC	Nd	1.50E-03	Nd
Mann-Whitney Test		Nd	$p = 1.76E-10$	Nd

Table S2.

Fosmid probes used for FISH. Fosmid names are taken from BACPAC resources (https://bacpac.chori.org/library.php?id=274)

Region	Name	Alternative name	Chr	coordinates (mm10)	
				Start (bp)	End (bp)
Ptn 5' end	WI1-1521J22	G135P601332D2	6	36843836	36881280
Ptn 3' end	WI1-2549N11	G135P600226B7	6	36597986	36643456
Sox6 5' end	WI1-870H24	G135P68352E1	7	116009901	116050430
Sox6 3' end	WI1-1204D22	G135P604872G2	7	115426587	115464203
Nrp1 5' end	WI1-2344M3	G135P61143B11	8	128311778	128356139
Nrp1 3' end	WI1-1336D24	G135P603048G1	8	128505666	128544645

Table S3.
Real-Time PCR Primers.

	Region	Oligo name	Sequence
Expression	*Ptn*	exp-mPtn-F	CGAGTGCAAACAGACCATGA
	Ptn	exp-mPtn-R	GGCGGTATTGAGGTCACATT
	Nrp1	exp-mNrp1-F	GGCCGATTCAGGACCATAC
	Nrp1	exp-mNrp1-R	ATAGACCACAGGGCTCACCA
	Sox6	exp-mSox6-F	GGATTGGGGAGTACAAGCAA
	Sox6	exp-mSox6-R	CATCTGAGGTGATGGTGTGG
	Itgb1	exp-mItgb1-F	AGATCCCAAGTTTCAAGGGC
	Itgb1	exp-mItgb1-R	TGAAGGCTCTGCACTGAACA
	Pard3	exp-mPard3-F	GTGTCCGTGGAGGTTCAAGT
	Pard3	exp-mPard3-R	TATGGAGCTGGCATTCTTCC
	Plekha7	exp-mPlekha7-F	TGGACAAAAGCTCAGAAGGG
	Plekha7	exp-mPlekha7-R	TGCTCTTGGGAAGACTCTGG
	Pou5f1	Oct4-F	CGAGAACAATGAGAACCTTC
	Pou5f1	Oct4-R	CCTTCTCTAGCCCAAGCTGAT
	Klf4	exp-mKlf4-F	GGCGAGAAACCTTACCACTGT
	Klf4	exp-mKlf4-R	TACTGAACTCTCTCTCCTGGCA
	FoxA2	exp-mFoxA2-F	CATCCGACTGGAGCAGCTA
	FoxA2	exp-mFoxA2-R	GCGCCCACATAGGATGAC
	Nestin	exp-mNestin-F	GATCGCTCAGATCCTGGAAG
	Nestin	exp-mNestin-R	AGGTGTCTGCAAGCGAGAGT
	Fgf5	exp-mFgf5-F	AAAACCTGGTGCACCCTAGA
	Fgf5	exp-mFgf5-R	CATCACATTCCCGAATTAAGC
	Gapdh	Gapdh-F	ATCACCATCTTCCAGGAGCGAG
	Gapdh	Gapdh-R	GACCCTTTTGGCTCCACCCTTC
ChIP / Replication Timing	*Ptn* promoter	RT-Ptn-4F	AGAGAAGAAGCAGGCTGTGC
	Ptn promoter	RT-Ptn-4R	GGGTGGGTGCTAAGAACAAA
	Nrp1 promoter	Prom-Nrp1-F1	TCTTTGCAACCCCTTGTACC
	Nrp1 promoter	Prom-Nrp1-R1	AAGGAGCTGGTGGGTAAGGT
	Sox6	gb-Sox6-F4	AATTGGGCCCCTCTTTCTCT
	Sox6	gb-Sox6-R4	TCTCTGCAAGGCTCTCAGGT
	Actb promoter	Actinf	CCTCGATGCTGACCCTCATCC
	Actb promoter	Actinr	GACACTGCCCCATTCAATGTCTC
	Clec2l	RT-Clec2l-F	TGCTGTGTCCTTGTCCTCAG
	Clec2l	RT-Clec2l-R	CTCAGCCCAGTCCTTGACTC
	Mgam	RT-Mgam-F	TTTTGCTGCTGTTTGCATTC
	Mgam	RT-Mgam-R	GATGCCTCCCACATTTCACT

References

1. P. Meister, A. Taddei, Building silent compartments at the nuclear periphery: A recurrent theme. *Curr. Opin. Genet. Dev.* **23**, 96–103 (2013). Medline doi:10.1016/j.gde.2012.12.001

2. A. Akhtar, S. M. Gasser, The nuclear envelope and transcriptional control. *Nat. Rev. Genet.* **8**, 507–517 (2007). Medline doi:10.1038/nrg2122

3. L. Guelen, L. Pagie, E. Brasset, W. Meuleman, M. B. Faza, W. Talhout, B. H. Eussen, A. de Klein, L. Wessels, W. de Laat, B. van Steensel, Domain organization of human chromosomes revealed by mapping of nuclear lamina interactions. *Nature* **453**, 948–951 (2008). Medline doi:10.1038/nature06947

4. L. E. Finlan, D. Sproul, I. Thomson, S. Boyle, E. Kerr, P. Perry, B. Ylstra, J. R. Chubb, W. A. Bickmore, Recruitment to the nuclear periphery can alter expression of genes in human cells. *PLOS Genet.* **4**, e1000039 (2008). Medline doi:10.1371/journal.pgen.1000039

5. K. L. Reddy, J. M. Zullo, E. Bertolino, H. Singh, Transcriptional repression mediated by repositioning of genes to the nuclear lamina. *Nature* **452**, 243–247 (2008). Medline doi:10.1038/nature06727

6. D. Peric-Hupkes, W. Meuleman, L. Pagie, S. W. Bruggeman, I. Solovei, W. Brugman, S. Gräf, P. Flicek, R. M. Kerkhoven, M. van Lohuizen, M. Reinders, L. Wessels, B. van Steensel, Molecular maps of the reorganization of genome-nuclear lamina interactions during differentiation. *Mol. Cell* **38**, 603–613 (2010). Medline doi:10.1016/j.molcel.2010.03.016

7. T. S. Mikkelsen, M. Ku, D. B. Jaffe, B. Issac, E. Lieberman, G. Giannoukos, P. Alvarez, W. Brockman, T. K. Kim, R. P. Koche, W. Lee, E. Mendenhall, A. O'Donovan, A. Presser, C. Russ, X. Xie, A. Meissner, M. Wernig, R. Jaenisch, C. Nusbaum, E. S. Lander, B. E. Bernstein, Genome-wide maps of chromatin state in pluripotent and lineage-committed cells. *Nature* **448**, 553–560 (2007). Medline doi:10.1038/nature06008

8. I. Hiratani, T. Ryba, M. Itoh, T. Yokochi, M. Schwaiger, C. W. Chang, Y. Lyou, T. M. Townes, D. Schübeler, D. M. Gilbert, Global reorganization of replication domains

during embryonic stem cell differentiation. *PLOS Biol.* **6**, e245 (2008). Medline doi:10.1371/journal.pbio.0060245

9. See supplementary materials on *Science* Online.

10. F. Zhang, L. Cong, S. Lodato, S. Kosuri, G. M. Church, P. Arlotta, Efficient construction of sequence-specific TAL effectors for modulating mammalian transcription. *Nat. Biotechnol.* **29**, 149–153 (2011). Medline doi:10.1038/nbt.1775

11. Q. Ding, Y. K. Lee, E. A. Schaefer, D. T. Peters, A. Veres, K. Kim, N. Kuperwasser, D. L. Motola, T. B. Meissner, W. T. Hendriks, M. Trevisan, R. M. Gupta, A. Moisan, E. Banks, M. Friesen, R. T. Schinzel, F. Xia, A. Tang, Y. Xia, E. Figueroa, A. Wann, T. Ahfeldt, L. Daheron, F. Zhang, L. L. Rubin, L. F. Peng, R. T. Chung, K. Musunuru, C. A. Cowan, A TALEN genome-editing system for generating human stem cell-based disease models. *Cell Stem Cell* **12**, 238–251 (2013). Medline doi:10.1016/j.stem.2012.11.011

12. J. Kind, L. Pagie, H. Ortabozkoyun, S. Boyle, S. S. de Vries, H. Janssen, M. Amendola, L. D. Nolen, W. A. Bickmore, B. van Steensel, Single-cell dynamics of genome-nuclear lamina interactions. *Cell* **153**, 178–192 (2013). Medline doi:10.1016/j.cell.2013.02.028

13. A. E. Carpenter, S. Memedula, M. J. Plutz, A. S. Belmont, Common effects of acidic activators on large-scale chromatin structure and transcription. *Mol. Cell. Biol.* **25**, 958–968 (2005). Medline doi:10.1128/MCB.25.3.958-968.2005

14. R. Eskeland, M. Leeb, G. R. Grimes, C. Kress, S. Boyle, D. Sproul, N. Gilbert, Y. Fan, A. I. Skoultchi, A. Wutz, W. A. Bickmore, Ring1B compacts chromatin structure and represses gene expression independent of histone ubiquitination. *Mol. Cell* **38**, 452–464 (2010). Medline doi:10.1016/j.molcel.2010.02.032

15. D. S. Dimitrova, D. M. Gilbert, The spatial position and replication timing of chromosomal domains are both established in early G1 phase. *Mol. Cell* **4**, 983–993 (1999). Medline doi:10.1016/S1097-2765(00)80227-0

16. I. Thomson, S. Gilchrist, W. A. Bickmore, J. R. Chubb, The radial positioning of chromatin is not inherited through mitosis but is established de novo in early G1. *Curr. Biol.* **14**, 166–172 (2004). doi:10.1016/j.cub.2003.12.024

17. R. R. Williams, V. Azuara, P. Perry, S. Sauer, M. Dvorkina, H. Jørgensen, J. Roix, P. McQueen, T. Misteli, M. Merkenschlager, A. G. Fisher, Neural induction promotes large-scale chromatin reorganisation of the Mash1 locus. *J. Cell Sci.* **119**, 132–140 (2006). Medline doi:10.1242/jcs.02727

18. I. Hiratani, T. Ryba, M. Itoh, J. Rathjen, M. Kulik, B. Papp, E. Fussner, D. P. Bazett-Jones, K. Plath, S. Dalton, P. D. Rathjen, D. M. Gilbert, Genome-wide dynamics of replication timing revealed by in vitro models of mouse embryogenesis. *Genome Res.* **20**, 155–169 (2010). Medline doi:10.1101/gr.099796.109

19. C. Morey, N. R. Da Silva, P. Perry, W. A. Bickmore, Nuclear reorganisation and chromatin decondensation are conserved, but distinct, mechanisms linked to Hox gene activation. *Development* **134**, 909–919 (2007). Medline doi:10.1242/dev.02779

20. Q. L. Ying, M. Stavridis, D. Griffiths, M. Li, A. Smith, Conversion of embryonic stem cells into neuroectodermal precursors in adherent monoculture. *Nat. Biotechnol.* **21**, 183–186 (2003). Medline doi:10.1038/nbt780

21. G. Guo, J. Yang, J. Nichols, J. S. Hall, I. Eyres, W. Mansfield, A. Smith, Klf4 reverts developmentally programmed restriction of ground state pluripotency. *Development* **136**, 1063–1069 (2009). Medline doi:10.1242/dev.030957

22. S. Chambeyron, W. A. Bickmore, Chromatin decondensation and nuclear reorganization of the HoxB locus upon induction of transcription. *Genes Dev.* **18**, 1119–1130 (2004). Medline doi:10.1101/gad.292104

23. S. Boyle, S. Gilchrist, J. M. Bridger, N. L. Mahy, J. A. Ellis, W. A. Bickmore, The spatial organization of human chromosomes within the nuclei of normal and emerin-mutant cells. *Hum. Mol. Genet.* **10**, 211–219 (2001). Medline doi:10.1093/hmg/10.3.211

24. Y. Hochberg, Y. Benjamini, More powerful procedures for multiple significance testing. *Stat. Med.* **9**, 811–818 (1990). Medline doi:10.1002/sim.4780090710

25. T. Ryba, D. Battaglia, B. D. Pope, I. Hiratani, D. M. Gilbert, Genome-scale analysis of replication timing: From bench to bioinformatics. *Nat. Protoc.* **6**, 870–895 (2011). Medline doi:10.1038/nprot.2011.328